Pergamon

Geochimica et Cosmochimica Acta, Vol. 68, No. 11, pp. 2577–2589, 2004

0016-7037/04 $30.00 + .00

doi:10.1016/j.gca.2003.10.044

The nature of molecular cloud material in interplanetary dust

Lindsay P. Keller,[1,*] Scott Messenger,[2,†] George J. Flynn,[3] Simon Clemett,[4] Sue Wirick,[5] and Chris Jacobsen[5]

[1]Mail Code SR, NASA Johnson Space Center, Houston, TX 77058, USA
[2]Laboratory for Space Sciences and Physics Department, Washington University, St. Louis, MO 63130, USA
[3]Department of Physics, SUNY Plattsburgh, Plattsburgh, NY 12901, USA
[4]Mail Code C23, Lockheed-Martin, NASA Johnson Space Center, Houston, TX 77058, USA
[5]Physics Department, SUNY Stony Brook, Stony Brook, NY 11794, USA

(*Received January* 22, 2003; *accepted in revised form October* 21, 2003)

Abstract—Eight interplanetary dust particles (IDPs) exhibiting a wide range of H and N isotopic anomalies have been studied by transmission electron microscopy, x-ray absorption near-edge structure spectroscopy, and Fourier-transform infrared spectroscopy. These anomalies are believed to have originated during chemical reactions in a cold molecular cloud that was the precursor to the Solar System. The chemical and mineralogical studies reported here thus constitute direct studies of preserved molecular cloud materials. The H and N isotopic anomalies are hosted by different hydrocarbons that reside in the abundant carbonaceous matrix of the IDPs. Infrared measurements constrain the major deuterium (D) host in the D-enriched IDPs to thermally labile aliphatic hydrocarbon groups attached to macromolecular material. Much of the large variation observed in D/H in this suite of IDPs reflects the variable loss of this labile component during atmospheric entry heating. IDPs with elevated $^{15}N/^{14}N$ ratios contain N in the form of amine ($-NH_2$) functional groups that are likely attached to other molecules such as aromatic hydrocarbons. The host of the N isotopic anomalies is not as readily lost during entry heating as the D-rich material. Infrared analysis shows that while the organic matter in primitive anhydrous IDPs is similar to that observed in acid residues of primitive chondritic meteorites, the measured aromatic:aliphatic ratio is markedly lower in the IDPs.

1. INTRODUCTION

Interplanetary dust particles (IDPs) collected in the Earth's stratosphere are fragments of asteroids and comets that are largely unsampled by collected meteorites (Bradley et al., 1988). Although the specific parent bodies of IDPs are unknown, the anhydrous chondritic-porous (CP) subset has been linked to a cometary source (Brownlee et al., 1995) and hydrated IDPs have been associated with asteroids (Bradley and Brownlee, 1992; Keller et al., 1992; Rietmeijer, 1992). Infrared spectra of the major phases in primitive anhydrous IDPs such as crystalline Mg-rich silicates, glass with embedded metal and sulfides (GEMS) (Bradley et al., 1999; Keller and Flynn, 2003), Fe-sulfides (Keller et al., 2002) and organics (Flynn et al., 2003) match spectral features of comets and young stellar objects. The CP IDPs are the most primitive extraterrestrial materials available for laboratory study based on their unequilibrated mineralogy (Bradley, 1994; Keller et al., 2000), chemistry (Thomas et al., 1993; Flynn et al., 1993), and isotopic signatures (McKeegan et al., 1985; Messenger and Walker, 1997; Messenger, 2000; Aléon et al., 2001). In particular, CP IDPs escaped the thermal processing and water-rock interactions that modified the original mineralogy and chemistry of even the most primitive meteorites. Such IDPs may constitute pristine aggregates of nebular and presolar materials, likely preserving some interstellar phases that have not survived in meteorites.

Presolar materials are abundant in IDPs, including recently discovered discrete grains of silicate stardust (Messenger et al., 2003b) and molecules that formed in a cold molecular cloud environment (Messenger, 1997; Messenger and Walker, 1997). These phases are known to have an extrasolar origin because of their anomalous isotopic compositions, as determined by secondary ion mass spectrometry (SIMS). The isotopic signatures of the stardust grains reflect the underlying nucleosynthetic processes of their parent stars. In contrast, molecular cloud materials are marked by extreme enrichments in deuterium (D) and ^{15}N that likely result from mass fractionation during very low temperature (10–100 K) chemical reactions (chemical fractionation).

There is strong support for an interstellar origin of the high D/H ratios observed in meteorites and IDPs. Deuterium is quickly consumed as nucleosynthetic fuel in stars and its spallogenic formation is not significant. Owing to the large difference in the masses of its isotopes, H is easily fractionated during chemical processes, especially at low temperatures. Extremely large H isotopic fractionation is observed in cold interstellar molecular clouds, where D/H ratios of simple molecules reach 10^{-2} to 10^{-1} compared to the local Solar System average of $\sim 10^{-5}$ (Millar et al., 1989). Sandford et al. (2001) have argued that selective photodissociation of polycyclic aromatic hydrocarbon (PAH) molecules could also significantly fractionate H in the diffuse interstellar medium.

The origin of the ^{15}N enrichments is less certain because ^{15}N-rich molecules have yet to be observed in cold interstellar clouds, although highly enriched ^{15}N organic molecules have been detected recently in comets using UV spectroscopy measurements (Arpigny et al., 2003). Nitrogen isotopic fractionation has not historically received much attention in interstellar chemical models. However, two recent studies have provided

* Author to whom correspondence should be addressed (lindsay.p.keller@jsc.nasa.gov).
† *Present address:* Mail Code SR, NASA Johnson Space Center, Houston, TX 77058.

some theoretical basis for the interstellar origin of ^{15}N enrichments. Firstly, Terzieva and Herbst (2000) investigated the N isotopic fractionation in a variety of relevant gas phase reactions, finding a maximum of 25% enrichment in ^{15}N. Secondly, Charnley and Rodgers (2002) have proposed that ^{15}N-rich NH_3 is efficiently formed during the last stages of molecular cloud evolution, reaching 80% enhancement in ^{15}N. However, the origin of N isotopic anomalies is complicated by the possible contribution of nucleosynthetic N (e.g., from stardust). This heightens the importance of determining the N-bearing phases present in ^{15}N-rich samples.

Hydrogen and N isotopic anomalies are common and highly variable among IDPs, with values eclipsing those observed in meteorites (Stadermann et al., 1999; Messenger, 2000). The D-rich phases in meteorites are known to include a wide range of organic molecules and water of hydration in some cases (Messenger and Walker, 1997, and references therein). Previous studies comparing the secondary ion signals of major elements (e.g., H, C, O) to D/H ratios within IDPs have shown that the major D-rich phases are carbonaceous (McKeegan et al., 1985; Aléon et al., 2001). However it is not possible to identify specific chemical compounds by SIMS, and the extremely small sizes of IDPs (~1 ng) has precluded the combined molecular and isotopic analyses that have been performed on meteorites.

Here we report the results of coordinated isotopic and chemical analyses of IDPs by a wide variety of techniques, including transmission electron microscopy (TEM), X-ray absorption near-edge structure (XANES) spectroscopy, Fourier transform infrared spectroscopy (FTIR), and electron energy-loss spectroscopy (EELS). We also describe detailed observations of two IDPs that exhibit higher D/H ratios than any known solar system materials. By comparing and contrasting the chemical signatures and isotopic compositions of a variety of IDPs, we infer the general characteristics of pristine molecular cloud material and define principal differences with organic phases observed in primitive meteorites.

2. EXPERIMENTAL TECHNIQUES

2.1. Sample Preparation

The particles studied here were provided by the Cosmic Dust Curatorial Facility at Johnson Space Center. The particles were collected by inertial impact on silicone oil-coated plastic plates deployed on the wings of a NASA WB57 aircraft which flew at a collection altitude of ~18 km. After being removed from the collector surface, each particle was individually cleaned of collector (silicone) oil with a hexane wash. The particles are assigned a name according to the collector they are recovered from and a particle index (e.g., L2008H9 was derived from large area collector L2008). Three of the particles are individual IDPs (L2008H9, L2008G12, and L2011R11), while the remaining particles studied are fragments of different IDPs that broke apart upon impacting the collector surface. Such particles are initially observed as clusters of material on the IDP collectors and are called 'cluster' IDPs (Table 1).

Two different protocols were followed for the samples after cleaning. The first set of samples (L2008H9, L2005*A3, L2008G12, L2011*B5, L2009*E2, L2011R11) were embedded in elemental sulfur (Bradley et al., 1993) and thin sections were obtained using an ultramicrotome equipped with a diamond knife. The thin sections (~70 nm thick) were placed on Cu TEM grids with either amorphous C or amorphous SiO substrates. The remaining material (typically ~50% of the original mass) was extracted from the S bead and transferred to an ion probe sample mount. For the second set of samples (L2009D11 and L2005#4), the particles were dry transferred with a tungsten needle to a Au substrate and pressed in with a spectroscopic grade quartz disk for ion microprobe analysis. Following the ion probe measurements, a (~200 × 200 μm) region of the Au mount surrounding each IDP was extracted with a scalpel by hand and attached to an epoxy microtome mount. Most of the Au surrounding the IDP was trimmed away with a glass knife in an ultramicrotome. It is important to note that the particle was undisturbed during the extraction and preparation for embedding and slicing. Finally, the particles (and surrounding Au) were embedded in S, and ultramicrotome sections were obtained following the same procedures described above. However, the microtome section thickness was reduced to ~30 nm to keep the Au from deforming around the particle. We used the second sample preparation method because it was the only way to preserve the petrographic context among the various datasets. This procedure allows for a direct one-to-one comparison of regions in ion images, TEM images, and X-ray absorption images obtained through XANES spectroscopy.

2.2. Ion Microprobe

2.2.1. Hydrogen Isotopes

All isotopic measurements were performed by SIMS with the Washington University modified CAMECA IMS-3f ion microprobe. The procedures used here closely followed those described in detail by McKeegan et al. (1985). Hydrogen isotopes were measured as negative secondary ions produced by a 1- to 5-nA, 16-keV Cs^+ primary ion beam at low mass resolving power. The Cs^+ beam was centered on each IDP and then slightly defocused. A small field aperture was used to restrict secondary ion transmission to a 15- to 20-μm area of the sample surface to minimize the contribution from background. In negative secondary ions, the contribution of H_2^- to the D^- peak is negligible. A typical measurement consisted of 15 to 25 cycles, where the H^- and D^- ions are alternatively measured in an automated peak-jumping mode. The H^- and D^- peaks are re-centered on the exit slit of the mass spectrometer every 5 cycles, though the peak shifts during a 5- to 10-min measurement are typically negligible. Terrestrial amphibole grains similar in size to the IDPs, and pressed nearby into the Au were used as isotopic standards to correct for instrumental mass fractionation. For the smallest grains, or those with particularly low D^- signal, the H^- and D^- peak positions were determined on the standard and only the H^- was centered on the sample. Shifts in the position of the H^- peak tracked during the measurement were then applied to the D^- peak.

All particles with D/H exceeding twice the terrestrial SMOW (standard mean ocean water) value ($D/H_{SMOW} = 1.5576 \times 10^{-4}$) were subjected to H isotopic imaging to determine whether there was significant μm-scale isotopic heterogeneity in the samples. For these measurements, a ~5-nA Cs^+ beam was defocused to ~50 μm over the particles. When there was sufficient signal, a contrast aperture was employed to improve the spatial resolution of the images, which reached ~1 μm under favorable circumstances. The secondary ions were imaged directly onto a multichannel plate coupled to a fluorescent screen, exploiting the capability of the IMS-3f to act as an ion microscope. The optical image appearing on the fluorescent screen was digitized with a 16-bit Photometrics 200 series CCD camera controlled with a Silicon Graphics workstation. The exposure times for H^- and D^- images were chosen to optimize the dynamic range in the images while avoiding saturation. The non-linearity of the MCP was corrected for when deriving isotopic ratios from the images by using the formula $\frac{D}{H} = \left(\frac{I_D}{I_H} \cdot \frac{T_H}{T_D}\right)^N$, where N was determined by running a variety of standard image exposures. The techniques for quantifying ion images with the Washington University ion microprobe were largely developed by Nittler (1996).

2.2.2. Nitrogen Isotopes

Nitrogen isotopes were measured as negative secondary ions at high mass resolving power ($m/\Delta m \sim 4500$) closely following previously established procedures (McKeegan et al., 1985). To correct for instrumental mass fractionation and establish initial peak positions, we used 5- to 10-μm fragments of the terrestrial standard 1-hydroxy benzotriazole hydrate. As with the H isotopic measurements, a small field

aperture was combined with a slightly defocused beam to minimize contribution from the background. Secondary ions were collected through a 30-V energy window, where the low energy edge of the ion energy distribution was continuously monitored during the measurement to compensate for sample charging.

2.3. Transmission Electron Microscopy

We used two TEMs in this study, a JEOL 2010 (200 kV) TEM equipped with a Noran thin-window energy-dispersive X-ray (EDX) spectrometer and a Gatan parallel electron energy-loss spectrometer (PEELS), and a JEOL 2000FX (200 kV) with a Link thin-window EDX spectrometer. Mineral identifications were based on electron diffraction data from zone axis orientations combined with quantitative EDX analyses. Quantitative EDX analyses were obtained using standard Cliff-Lorimer techniques utilizing *k*-factors obtained from well-characterized standards. Dark-field imaging techniques were used to determine solar flare track densities and to search for irradiated/sputtered rims.

The bonding states and distribution of C and N were investigated using EELS through the analysis of the *k*-edge fine structure (spectrum shape, relative intensities of features, and peak positions) compared to well-characterized standards. The C *k*-edge EELS data were obtained on microtome sections of IDPs that had been embedded in S, sectioned, and placed on amorphous SiO substrates. In this way, we could exclude any contribution from the substrate or C-based epoxies. The S beads are attached to standard epoxy microtomy mounts using cyanoacrylate adhesives. The C and N *k*-edges for C≡N are very distinctive, so we can also exclude any contribution to the data from this source. EELS spectra were collected using the TEM in image mode at 200 keV with a 1-mm entrance slit to the spectrometer and an energy dispersion of 0.1 eV/channel. The spectrometer and TEM were optimized for high spectral resolution (0.7 eV full-width at half-maximum at the zero-loss peak). EELS spectra were collected for 5 to 100 s from regions that were typically 50 to 100 nm in diameter. All of the spectra were calibrated by setting the energy of the π-π^* feature in the C *k*-edge to 285 eV. We compared the IDP spectra to EELS data obtained from phase pure synthetic materials (Keller, 1998).

2.4. Fourier-Transform Infrared Spectroscopy

All of the FTIR measurements were obtained using synchrotron-based instruments on beamlines U10B and U4IR at the National Synchrotron Light Source, Brookhaven National Laboratory. The synchrotron light source provides over 100 times the brightness of conventional globar sources. Transmission FTIR spectra were collected using Nicolet Continuum and Irus FTIR microscopes over the wavelength range of 4000 to 650 cm^{-1} with apertures selected to maximize the signal while minimizing scattering effects. We collected spectra directly from microtome thin sections of the IDPs on thin amorphous C substrates. The samples and the microscope were continuously purged with dry N_2. Background spectra were acquired from the substrate film immediately adjacent to the IDP section. Final baseline corrected and smoothed spectra were obtained by subtracting the background from the sample spectrum. Between 1000 and 4000 scans (interferograms) were averaged for each specimen with a spectral resolution of 4 cm^{-1}. For the FTIR data shown here, we have normalized the band depth to the strength of the Si-O stretch at ~1000 cm^{-1}, even though the particles studied have variable proportions of crystalline and amorphous silicate material which can affect the measured silicate band depth.

2.5. X-Ray Absorption Near-Edge Structure Spectroscopy

We used the scanning transmission X-ray microscope (STXM) at beamline X1A of the National Synchrotron Light Source (Brookhaven National Laboratory) to map the distribution of C in ultramicrotome thin sections of IDPs and to investigate the C-bonding environment in the samples using X-ray absorption near-edge structure (XANES) spectroscopy. While generally similar to the EELS measurements (the same physical process governs both techniques), XANES offers increased energy-resolution by using monochromatic X-rays (0.1 eV as opposed to 0.7 eV for the EELS measurements). The high-resolution of the XANES measurements allows for the detection and quantification of spectral features resulting from different bond environments that are unresolved in the EELS spectra. The XANES measurements are made directly on ultramicrotome thin sections of IDPs embedded in S and placed on SiO thin films supported by Cu TEM grids. Additional experimental details of the XANES measurements are given in Flynn et al. (2003).

3. RESULTS

Since the first experiments were performed in this study, the analytical techniques have steadily improved, and the sample protocol has evolved accordingly. Although this suite of particles shows widely varying H and N isotopic compositions, their overall mineralogy and petrography are similar. All of these particles belong to the anhydrous, CP subset of IDPs. The mineralogy of the anhydrous IDPs is distinct from primitive meteorites and is dominated by Mg-rich crystalline silicates (mostly enstatite with minor forsterite), Fe-Ni sulfides (mostly pyrrhotite), and GEMS (glass with embedded metal and sulfides; Bradley, 1994). The mineral grains and glassy objects are supported by a ubiquitous carbonaceous matrix that surrounds and binds the individual grains. The carbonaceous matter is abundant in these particles and appears amorphous in high-resolution TEM images and diffraction patterns. Vesicular carbon is observed in several IDPs that have been strongly heated during atmospheric entry.

Bulk chemical compositions of five of the particles have been measured using SEM-EDX techniques (Thomas et al., 1993) and all major element concentrations are within a factor of two of CI values except for C which ranges from ~2 to 13 × CI (Table 2).

The C-XANES spectra are generally quite similar for the particles discussed here. The C-rich areas in most IDPs have C-XANES spectra that show two strong absorption features, one at ~285 eV, from the C=C in a ring structure, and the second at ~288.5 eV, from C=O. A third weaker absorption feature, at ~286.5 eV is also observed, but has not been definitively associated with a specific functional group. The variations in the relative strengths of the 285- to the 288.5-eV absorption features indicate that the ratio of C=C to C=O is not constant from one IDP to another (Flynn et al., 2003).

FTIR measurements show a distinct 10-μm Si-O stretch from the silicates in the particles and a group of absorption features between 3000 and 2800 cm^{-1} that correspond to the CH_2 and CH_3 symmetric and asymmetric stretches in aliphatic hydrocarbons. The C-H band positions are similar among the analyzed particles, but the intensity varies widely (Fig. 1). The C-H stretches were not detected in L2009*E2 and L2005#4 because of low sample mass. In pure aliphatic hydrocarbons, the C-H stretches appear as four resolved peaks whereas in materials where the aliphatic groups are bound to strongly perturbing groups (e.g., aromatic molecules), the two lowest frequency bands blend into a single band (Sandford et al., 1991). The IDP spectra are consistent with the presence of aliphatic groups attached to other molecules.

The extent of atmospheric entry heating on these IDPs has been determined through several independent observations, including the development of magnetite rims, the microstruc-

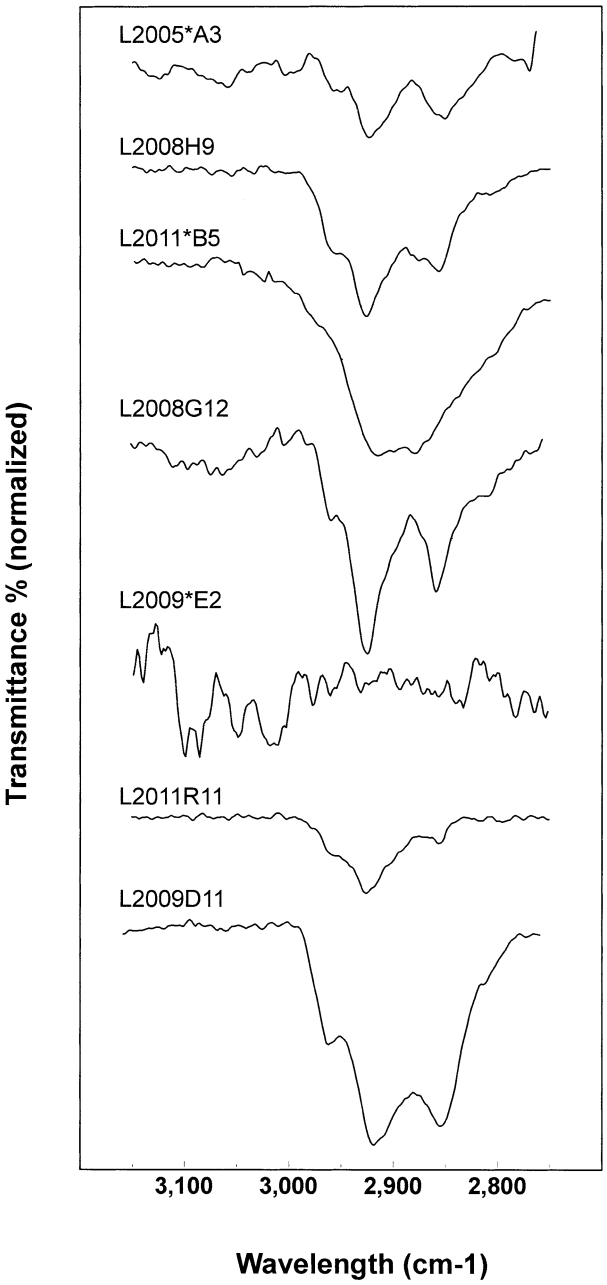

Fig. 1. FTIR transmission spectra showing the C-H stretch region for the suite of anhydrous IDPs. The intensity of the C-H features are normalized to the band depth of the silicate feature at ~1000 cm^{-1}.

ture of the carbonaceous material (graphitization, vesiculation, etc.), and the observation of solar flare tracks in crystalline silicates. Fraundorf et al. (1982) have previously determined that solar flare tracks in crystalline silicates are annealed when peak temperatures exceed ~600°C. IDPs lacking any observable tracks are considered to be severely heated, whereas those possessing tracks but exhibiting distinct magnetite rims have been moderately heated. Particles lacking any indicators of atmospheric entry heating are inferred to have escaped significant heating.

Below we summarize the distinguishing mineralogical and organic features of particles arranged according to their H isotopic compositions.

3.1. Observations of an IDP With Very Low D/H (L2005*A3)

L2005*A3 has the lowest D/H ratio among the IDPs studied here (−420 ± 20‰) and has one of the lowest D/H ratios ever observed in IDPs. This particle is from an unusually D-rich cluster IDP (L2005 #31), with associated fragments reaching δD values of 20,000 to 50,000‰. L2005*A3 also exhibits a very high bulk $\delta^{15}N$ excess of 400‰. All five other fragments from this cluster are also ^{15}N-rich, with values ranging from 260 to 480‰. This fragment has undergone strong heating during atmospheric entry as evidenced by a thick, nearly continuous magnetite rim (Fig. 2) and a lack of solar flare tracks. FTIR measurements show a distinct 10-μm Si-O stretch from the silicates in the particle and a weak group of aliphatic absorption features between 3000 and 2800 cm^{-1}.

EELS data for the C *k*-edge show a broad π^* feature that can be deconvolved into at least two distinct features that we interpret as evidence for multiple ring structures (Fig. 3). We found that N is associated with the carbonaceous material based upon a distinct N *k*-edge at ~400 eV in EELS spectra. Background-subtracted spectra of the N *k*-edge in L2005*A3 and several N standards are presented in Figure 4. A comparison of the L2005*A3 spectra to the standards shows that the major N-bearing component in the IDP is most similar to the spectrum from an organic compound containing only N-H (amine) nitrogen. XANES data for other N-H bearing organic molecules show similar edge structure and peak positions (Franke et al., 1995). The L2005*A3 spectrum is distinctly different from those of nitrides, nitrate, and cyano-nitrogen (C≡N). Additionally, the edge shape and position are also inconsistent with spectra for gas phase N_2 and NH_3 (Berger et al., 1989).

3.2. Observations of IDPs With Terrestrial D/H (L2008H9, L2008G12 and L2011*B5)

Three of the particles studied here have δD values that fall within the range observed among terrestrial rocks (−200 to

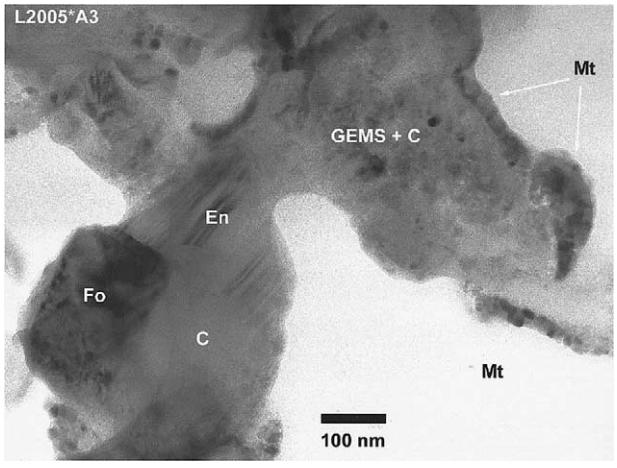

Fig. 2. A low magnification TEM image of a part of an ultramicrotome thin section of IDP L2005*A3 showing a polycrystalline magnetite rim formed during atmospheric entry heating.

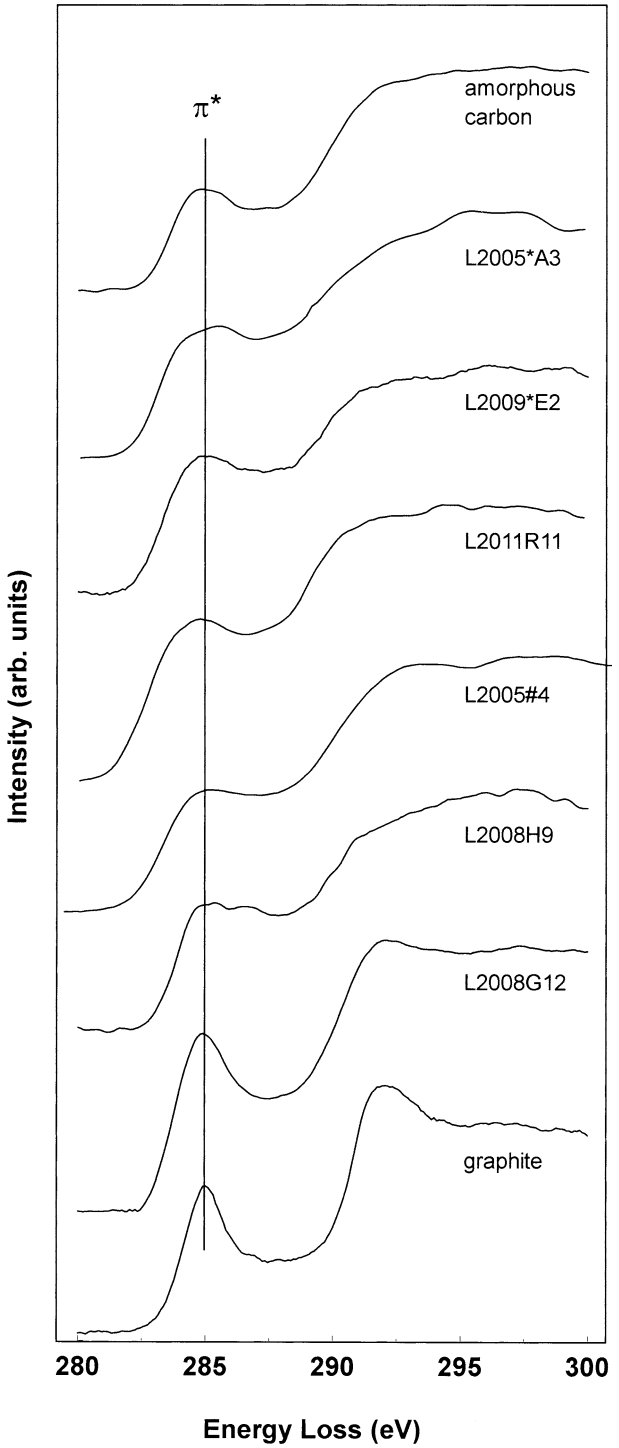

Fig. 3. EELS spectra at the carbon *k*-edge for a suite of anhydrous IDPs long with amorphous carbon (top) and graphite standards (bottom). The vertical line through the spectra at 285 eV indicates the peak that results from the π-π* transition in carbon ring structures.

+50‰). L2008 H9 has a relatively low δD of −122 ± 42‰. This is a compact particle that contains unusually abundant enstatite whiskers and platelets together with the typical mineralogical components of anhydrous IDPs. It is difficult to determine whether this particle was strongly heated during atmospheric entry, as there is no development of magnetite on the exposed surfaces (suggesting little heating), yet we were unable to find solar flare tracks in the crystalline silicates (suggesting strong heating). The EELS data show an edge that is largely consistent with amorphous C, although there is splitting of the π* peak which may indicate that multiple ring structures are present (Fig. 3). Nitrogen was not detected in this particle using EELS. The XANES data confirm that the carbonaceous material in L2008H9 is a mixture of aromatic carbon and other organic carbons, based on the presence of a major C=O feature at 288.5 eV (Fig. 5). FTIR spectra obtained from thin sections of L2008H9 show distinct features around 2800 to 3000 cm^{-1} that are consistent with the CH_2 and CH_3 stretching vibrations in aliphatic hydrocarbons (Fig. 1), and a weak feature at ~1700 cm^{-1} from the carbonyl functional group.

L2008G12 is the most C-rich IDP analyzed in this study. SEM-EDX bulk analyses show a bulk C content of ~44 atom

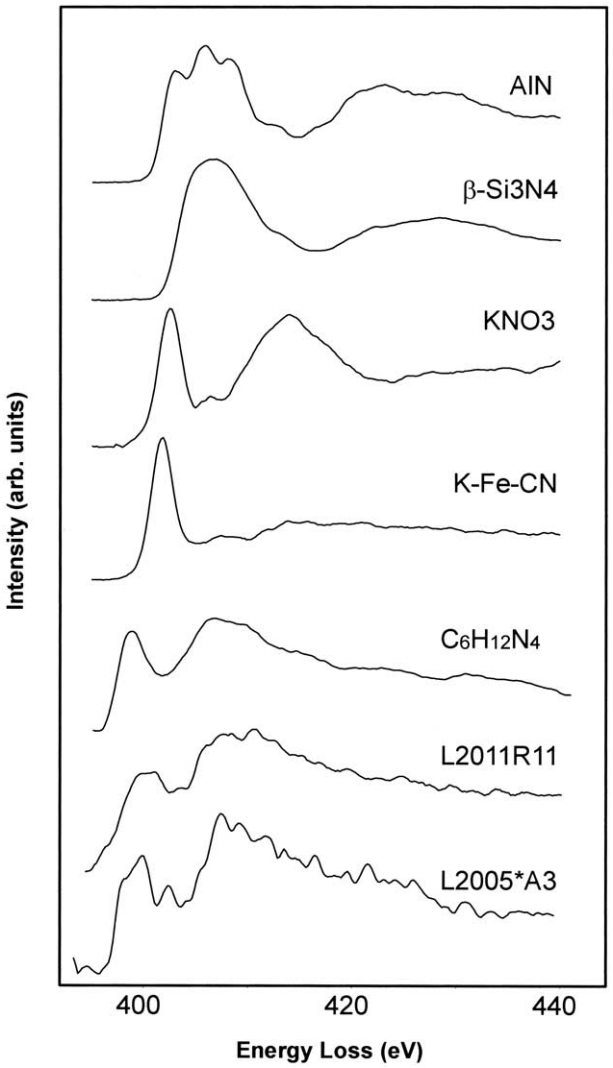

Fig. 4. EELS spectra at the nitrogen *k*-edge for the two IDPs showing detectable nitrogen in their carbonaceous matrices. The other spectra are from standards with different bonding environments for the N. The IDP spectra most closely match the N edge dominated by amine (-NH_2) nitrogen (spectrum labeled $C_6H_{12}N_4$).

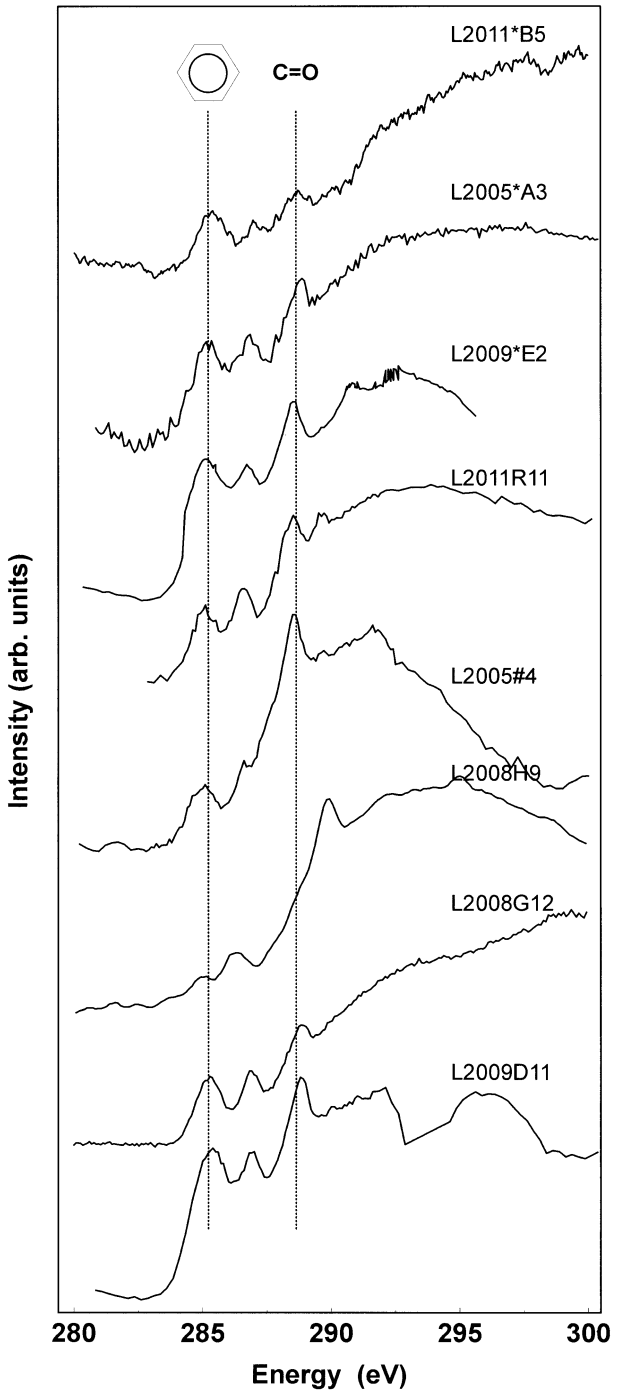

Fig. 5. XANES spectra at the carbon *k*-edge for the eight anhydrous IDPs analyzed in this study. The aromatic (carbon in ring structures) and carbonyl (C=O) features are indicated with the vertical lines.

% (Table 1). The measured δD (−56 ± 150‰) is within the range of terrestrial values. Mineral grains including enstatite, kamacite, Fe-carbides and Fe-sulfides are a minor component of the particle and are widely dispersed. The Fe-carbides are dominated by cohenite (Fe_3C) with 5- to 10-nm thick rims of well-crystallized graphite (Fig. 6). Carbon *k*-edge EELS spectra from the typical carbonaceous matter in L2008G12 show the development of fine structure consistent with poorly-graphitized carbon (Fig. 3). There is extensive vesiculation of the carbon at the ~5-μm scale and additional vesiculation at a much finer (10–100 nm) scale (Fig. 7). The particle morphology combined with a lack of solar flare tracks in the silicates, and the carbide-graphite assemblage is consistent with strong atmospheric entry heating. FTIR spectra from thin sections of L2008G12 (Fig. 1) show distinct features for the CH_2 and CH_3 stretching vibrations in the 2800- to 3000-cm^{-1} region as well as a distinct C=O feature centered at 1725 cm^{-1}. Several FTIR spectra show a broad, weak feature at ~3060 cm^{-1} which is consistent with the C-H stretching vibration in aromatic hydrocarbons (Fig. 8). XANES spectra from L2008G12 have a high energy shoulder on the 285-eV absorption, consistent with some amorphous elemental C mixed with the typical organic C observed in other IDPs (Fig. 5).

L2011*B5 has a bulk δD of –100 ± 35‰. This fragment has undergone moderate heating during atmospheric entry that has produced a discontinuous magnetite rim on the outer surface of the IDP, however, the crystalline silicates still retain solar flare tracks (~3×10^{10}/cm^2). In one of the lobes of the particle there is evidence for partial hydration in the form of poorly crystalline phyllosilicates replacing the amorphous glass in GEMS. Based on the particle petrography, it is unclear if this hydration occurred before or after atmospheric entry. The XANES spectra from L2011*B5 show the characteristic three peaks seen in typical IDP organic matter (Fig. 5). The FTIR spectra from L2011*B5 show weak absorptions in the C-H stretching region consistent with aliphatic hydrocarbons (Fig. 1).

3.3. Observations of IDPs With Moderate D-Enrichments (L2009*E2 and L2011R11)

L2009*E2 is a “classic” chondritic-porous (CP) anhydrous IDP, i.e., a high porosity particle containing submicrometer-sized mineral grains and GEMS grains bound together by abundant carbonaceous matrix. Ion microprobe measurements show a modest bulk δD of ~+400‰, although related fragments from the same cluster (L2009, cluster 7) show δD as high as +11,000‰ (Messenger and Walker, 1997; Messenger, 2000). L2009*E2 has been only slightly affected by atmospheric entry heating; while minor magnetite is observed on some surfaces, the presence of solar flare tracks in olivine and pyroxene indicate that this fragment of the cluster was not strongly heated during entry. The solar flare track density measured in multiple grains is ~5×10^{10}/cm^2. Low-Ca pyroxene (En > 98) is common and occurs in several morphologies including platelets, ribbons, and more rarely in rounded aggregates with forsterite (Fo95). The enstatite ribbons have aspect ratios up to 5. These distinctive pyroxene morphologies are believed to result from vapor-phase crystal growth (Bradley et al., 1983). Fe-Ni sulfide grains are <0.1 μm in size, and occur as discrete grains embedded in carbonaceous material and as inclusions within GEMS. A weak N edge is apparent in some EELS spectra from the carbonaceous material that suggests the presence of minor N present as the amine functional group (Keller et al., 1997). Flynn et al. (1999) obtained high resolution XANES spectra of the carbon speciation in a thin section of L2009*E2 and found that organic C was heteroge-

Table 1. IDPs analyzed in this study, their H and N isotopic compositions, solar flare track density (tracks/cm^2) and estimates of the degree of atmospheric entry heating experienced by the particles (n.m. = not measured, n.d. = not detected).

IDP	δD	δ^{15}N	Track density	Entry heating
L2005*A3	−417 (±24)	+396 (±41)	n.d.	Strong
L2008H9	−122 (±42)	n.m.	n.d.	Moderate
L2008G12	−56 (±150)	n.m.	n.d.	Strong
L2011*B5	−100 (±35)	n.m.	3×10^{10}	Low
L2009*E2	+392 (±117)	n.m.	5×10^{10}	Low
L2011R11	+200 (±50)	+250 (±20)	4×10^{10}	Moderate
L2009D11	+5,600 (±770)	n.m.	5×10^{10}	Low
L2005#4	+24,800 (±1500)	+338 (±78)	n.d.	Low

neously distributed in the amorphous C matrix at the micrometer-scale.

L2011R11 exhibits a significant δ^{15}N excess of 250‰ and a moderate δD excess of 200‰ (Messenger et al., 1996). A thin, discontinuous magnetite rim occurs on parts of the external surface of the particle, but pyroxene and olivine grains contain solar flare tracks with a track density of $\sim 4 \times 10^{10}$ cm^{-2} suggesting this particle has experienced moderate atmospheric entry heating. The carbonaceous material shows two distinct textures: (1) uniform, featureless regions up to ~0.1 μm in size; and (2) regions of vesicular carbon distributed throughout the particle.

Nitrogen is associated with the carbonaceous material in L2011 R11 based upon a distinct N *k*-edge at ~400 eV in the EELS spectra. Semiquantitative N analyses using EELS give an upper limit on the N/C atom ratio of ~0.1 (Keller et al., 1995), which is comparable to the chondritic value (N/C ~ 0.08, Anders and Grevesse, 1989). Since L2011R11 has a bulk C abundance of nearly 3 × CI, it is consequently enriched in N by a similar value. A typical background-subtracted spectrum of the N *k*-edge in L2011R11 is shown in Figure 4. The EELS data are most consistent with the bulk of the N in the form of N-H bonds. High-resolution TEM images and electron diffraction data of the carbonaceous material in L2011R11 show no evidence for crystalline N-bearing inclusions > 5 nm in size (such as nitrides). FTIR spectra from thin sections of L2011R11 help to further constrain the N speciation. A broad, weak band at ~3250 cm^{-1} in the spectra is consistent with N-H stretching vibrations (Fig. 1), but confirmation with the other main N-H absorption at ~1500 cm^{-1} is prohibited due to water bands. Features from C-N and C=N bonds are not observed in the FTIR spectra, although weak C-H stretching absorptions are present. The combined EELS and FTIR results indicate that the predominant N-speciation in L2011R11 is amine (-NH_2). These results have been confirmed by N-XANES measurements on the same particle (Feser et al., 2003). The XANES results also show a strong C=O feature at both the carbon and oxygen *k*-edges (Feser et al., 2003).

3.4. Observations of Extremely D-Rich IDPs (L2009D11 and L2005#4)

L2009D11 is a fragment from cluster particle 13 that showed a bulk δD of +5600‰. Hydrogen isotopic imaging of this IDP identified a 2- to 3-μm region with a δD value of at least 10,000‰. We used the modified sample preparation technique to prepare microtome thin sections of IDPs that have been pressed into gold and previously analyzed in the ion probe (see "Experimental Techniques"). TEM observation of the ultrami-

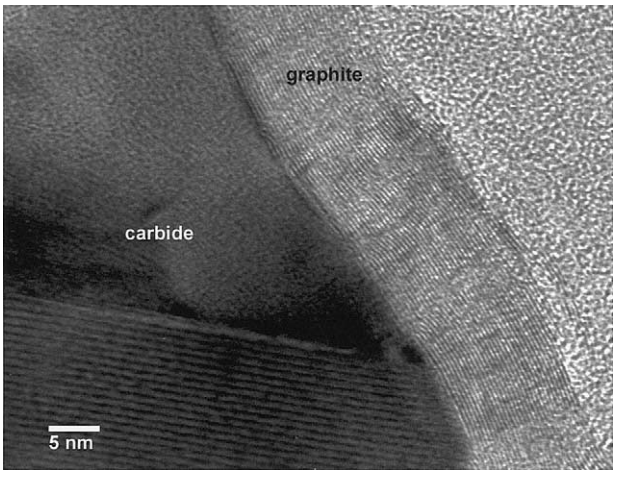

Fig. 6. A high-resolution TEM image of graphitic carbon rim ~10 nm thick surrounding a Fe-carbide grain in L2008G12. The graphite rims all show well-developed (002) lattice fringes.

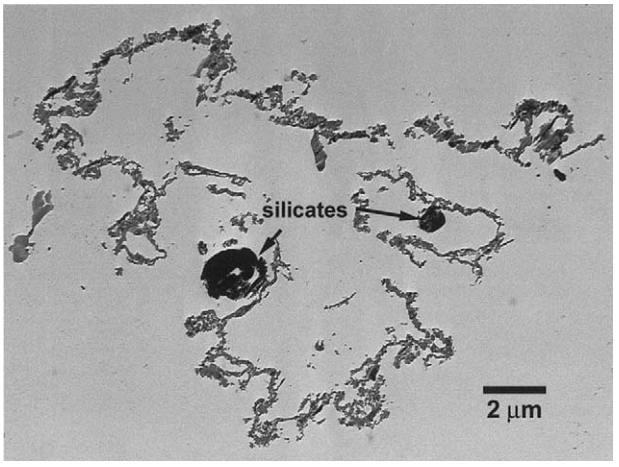

Fig. 7. A low magnification TEM image of an ultramicrotome thin section of L2008G12 showing its unusual internal structure. The high porosity of this particle likely developed in response to the loss of a volatile phase during atmospheric entry heating.

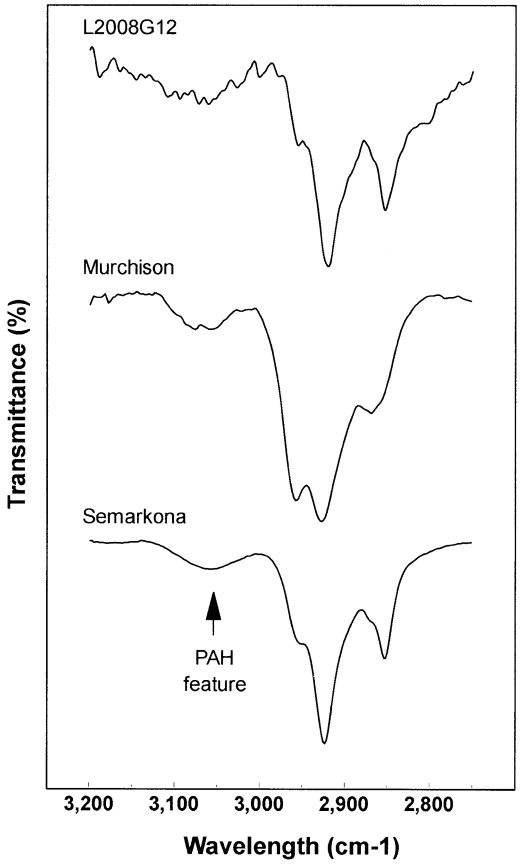

Fig. 8. FTIR spectra showing the C-H stretching region for acid residues from the Murchison and Semarkona meteorites compared to the anhydrous IDP L2008G12. All three materials show a pronounced features at ~3050 cm^{-1} that results from the C-H stretch in aromatic hydrocarbons. An FTIR spectrum showing the C-H stretching region for dibenzoperylene is also shown for comparison.

crotome thin sections of L2009D11 (20–30 nm thick) show that the particle is dominated by coarse-grained Fe-Ni sulfides and lesser crystalline silicates including enstatite, forsterite and anorthite. Solar flare tracks are observed in both the enstatite and anorthite, with track densities of $\sim 5 \times 10^{10}/cm^2$. Because of the way the sample was prepared, there is no ambiguity about the location of the D hotspot for the subsequent analyses (Fig. 9). The D hotspot region is dominated by poorly ordered carbonaceous material with embedded GEMS and fine-grained sulfides (Fig. 10). For the FTIR analyses, we used a small field-limiting aperture to confine the region of interest to the D hotspot. The FTIR spectra show solid state features for the silicate species in and around the hotspot and more importantly, reproducible features which correspond to the CH_2 and CH_3 stretching vibrations in aliphatic hydrocarbons (Fig. 1). FTIR spectra from the D-hotspot are similar (with respect to peak positions and relative band strengths) to the aliphatic hydrocarbons identified in other primitive anhydrous IDPs using IR techniques (Flynn et al., 2003). XANES spectra taken at the C *k*-edge show three major absorptions (Fig. 5) similar to those observed in previous analyses of D-rich material in IDPs, however, the C=O peak at 288.5 eV is not as intense as observed in other D-rich IDPs (see below), and the 285 eV peak is systematically broader in the L2009D11 hotspot spectra, which suggests that multiple carbon ring species are present.

L2005 #4 cluster 31 (cluster 31 is also the parent of L2005*A3) has a bulk δD of 24,800‰ and a $\delta^{15}N$ of 340‰. Minor phases include kamacite, magnetite, and a spinel grain embedded in Ca-aluminosilicate glass. Some of the petrographic context was lost when the IDP was crushed into the gold, and sputter-deposited Au complicates the TEM analysis. Nitrogen was detected in the carbonaceous material using EELS, but the concentration was too low to determine speciation. The distribution of carbonaceous material in a thin section of Dragonfly was mapped using the scanning transmission X-ray microscope (STXM) and XANES spectra were obtained

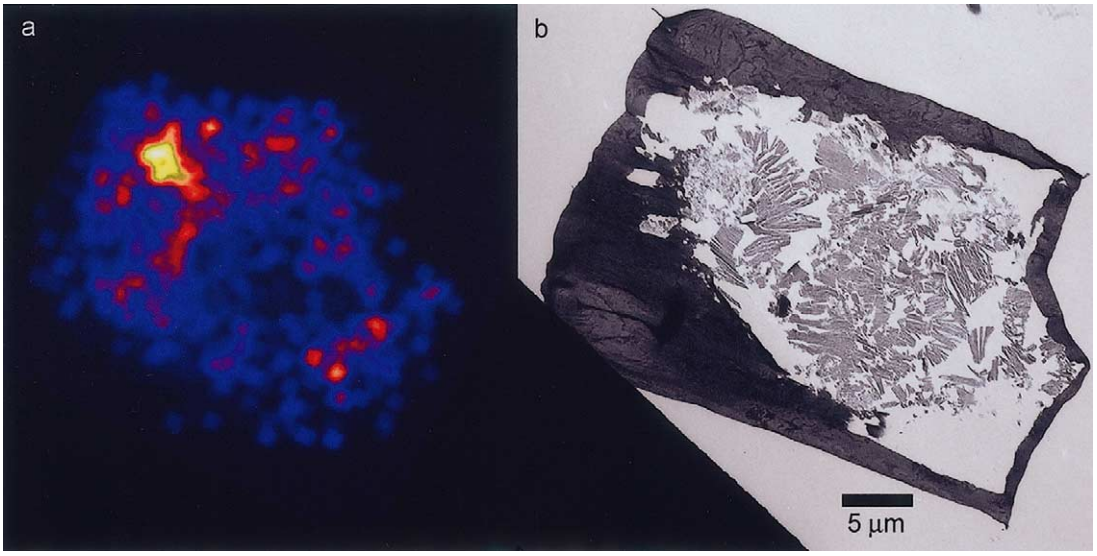

Fig. 9. (a) A false-color secondary ion image showing the spatial distribution of deuterium within IDP L2009D11. The high brightness area is a D hotspot ~3 μm in size. (b) A low magnification image of an ultramicrotome thin section of L2009D11 in the same orientation as the ion image in (a), showing the location in the thin section of the D-hotspot material.

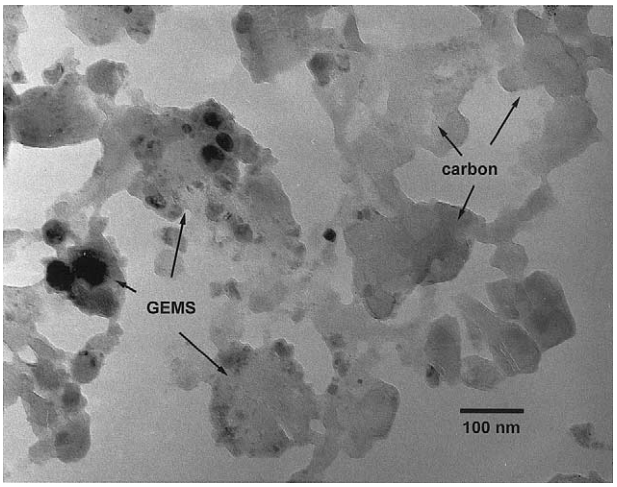

Fig. 10. A brightfield TEM image of the typical material that is observed within the D-hotspot in L2009D11. The hotspot is dominated by carbonaceous material (labeled "C"), with minor inclusions of mineral grains and GEMS.

at the C *k*-edge. The XANES data from points within the Dragonfly thin section are, in general, similar to other C-rich IDPs we have measured in that prominent C=C and C=O absorptions are observed (Fig. 5).

4. DISCUSSION

4.1. Implications for the Host of the Deuterium Enrichments in IDPs

Transmission electron microscopy and isotopic imaging of these IDPs show that the predominant H-bearing phase is the organic matrix material. None of these particles contain appreciable amounts of hydrated minerals, and H and C secondary ion images are closely correlated, in line with other studies of anhydrous IDPs (Aléon et al., 2001). The enormous variation in D/H observed between and within these IDPs further shows that the organic matter is composed of at least two isotopically distinct components. This variability in D/H ratios may be due to the loss of volatile D-rich components during atmospheric entry heating. This hypothesis is supported by the observation that IDPs with the largest D/H ratios have experienced minimal heating and those with low D/H have been most severely heated. Other than thermal processing during atmospheric entry, there are few systematic chemical or mineralogical differences between particles with elevated D/H and those with low D/H.

The least heated, most D-rich IDPs contain the least altered remnants of presolar molecular cloud materials. The importance of understanding the nature of this material is twofold: (1) these materials may closely resemble the precursors of primitive meteorite organics and (2) these materials likely represent the only direct solid samples of organic compounds formed in the ISM available for laboratory analysis.

Some primitive meteorites also contain D and ^{15}N-rich organic matter (Robert and Epstein, 1982; Kerridge, 1985). We compared the FTIR spectra obtained from acid insoluble resides from the Murchison CM carbonaceous chondrite and the Semarkona LL3 unequilibrated ordinary chondrite, with that obtained from D-rich and D-poor IDPs. Absorption features due to aliphatic CH_2 and CH_3 stretching vibrations as well as a broad aromatic C-H stretching feature at 3050 cm^{-1} are well resolved in the meteorite FTIR spectra (Fig. 8). Independent nuclear magnetic resonance measurements of the organic matter in Murchison acid residue show that the ratio of aromatic carbons to aliphatic carbons is ~60:40 (Cody et al., 2002). Our FTIR spectra from both Semarkona and Murchison meteorite residues are consistent with this estimate when the intrinsic band strengths for each of the hydrocarbon species are considered (Pendleton et al., 1995; Pendleton and Allamandola, 2002).

The C-H stretching features from aliphatic hydrocarbons are commonly detected in most C-rich IDPs, however, we have only detected aromatic hydrocarbons in one strongly heated IDP (L2008G12) to date using FTIR. The detection limits for aromatic hydrocarbons are poor given the intrinsic band strength and the signal to noise in the FTIR spectra from such small samples. Despite this limitation, we note that if most of our IDPs contained PAHs of a similar type and concentration as observed in the meteoritic acid residues, then the PAH feature would have been readily detected in the FTIR measurements. The absence of the aromatic C-H feature in the FTIR spectra shows that the IDP organic matter contains a substantially higher proportion of aliphatic functionality relative to low molecular weight PAHs in comparison to that observed in primitive meteorites. However, the XANES spectra also indicate a significant abundance of aromatic C from C-C π^* bonding resonance transitions. One possible resolution to this apparent contradiction is that much of the carbonaceous matter is comprised of very poorly graphitized carbon, possessing only short range order (<2 nm), or very large PAH molecules. It is possible that the organic matter in IDPs is similar to the original meteoritic organics that were subsequently affected by hydrothermal metamorphism. Such processes can result in the gradual degradation of aliphatic hydrocarbons into aromatic compounds. The aliphatic hydrocarbons in the meteorite residues are very similar to those in IDPs in terms of band positions and relative intensities. The one exception is the D-hotspot particle that has a lower CH_2/CH_3 band depth ratio, suggesting that the hydrocarbon chains are shorter than the meteoritic material.

Analysis of the D hotspot in L2009D11 provides additional insight into the nature of molecular cloud material. TEM investigations show that the D hotspot is localized within a region dominated by carbonaceous material. FTIR and XANES measurements further show that this D-rich carbonaceous matter contains both aliphatic and aromatic hydrocarbons. The FTIR spectra from the D-rich and D-poor fragments of separate cluster IDPs both show a Si-O absorption feature at ~1000 cm^{-1} and features which correspond to the CH_2 and CH_3 stretching vibrations of aliphatic hydrocarbons that occur in the 2800- to 3000-cm^{-1} region. However, the intensity ratio of the aliphatic feature relative to the silicate feature in the most D-poor fragment (L2005*A3) is ~25% of that observed in the D-rich fragment L2009D11. Although bulk composition data is unavailable for L2009D11, we estimate that the bulk carbon content is comparable to that observed in L2005*A3 based on TEM observations of microtome thin sections. Provided that these fragments each initially contained the same amount of

aliphatic material relative to the silicates, then the strong heating experienced by the D-poor particle could explain the loss of the aliphatics, or the conversion of the aliphatics into another form such as PAHs. The XANES spectra from the D-rich and D-poor fragments suggest a similar distribution of aromatic hydrocarbons. It is also interesting to note that although L2005*A3 is strongly depleted in D/H, it still retains a positive ^{15}N anomaly comparable in magnitude to the five other D-rich fragments analyzed from its parent cluster IDP. While it is possible that the putative volatile D-rich phase is also ^{15}N-rich, the evidence of strong heating clearly shows that a major host of the ^{15}N enrichment is a more refractory phase.

The identification of aliphatic groups as a major carrier of D in these particles has interesting astrophysical implications. The organic component of interstellar dust in the diffuse interstellar medium (ISM) is dominated by hydrocarbons (both aliphatic and aromatic forms) with little or no O in attached functional groups such as carbonyl and alcohols (Pendelton and Allamandola, 2002). The C-H stretching features of aliphatic hydrocarbons are observed along many lines of sight in the diffuse ISM (Ehrenfreund et al., 1991; Sandford et al., 1991; Whittet et al., 1997, Chiar et al., 2000). The situation is different in dense molecular clouds where the aliphatic features are not nearly as prominent (Allamandola et al., 1992). In dense clouds, UV irradiation as well as cosmic ray bombardment destroy aliphatic material through dehydrogenation, and the growth of ice mantles prevents the formation of new aliphatic materials (Mennella et al., 2002; Shenoy et al., 2003). Thus, we are faced with the following dilemma: we have identified aliphatic hydrocarbons as a major host of the D/H isotopic anomalies, yet these materials are not stable in the environment where they acquired their elevated D/H ratios. There are at least two resolutions to this apparent problem. The first is that exchange occurs rapidly between D-enriched ices and the organics encased by those ices, so that interstellar aliphatic hydrocarbons may have acquired their elevated D/H ratios in this manner (Bernstein et al., 1999; Sandford et al., 2000, 2001). The second is through UV photolysis of PAHs in H_2O ices which produces partially hydrogenated aromatic hydrocarbons (Bernstein et al., 1999). Hydrogen addition to the edges of PAHs results in the formation of aliphatic side groups and cyclic aliphatic hydrocarbons replacing aromatic rings. Furthermore, H exchange can enrich these complex molecules in D.

4.2. Implications for the Hosts of the ^{15}N Enrichments in IDPs

Like C, N is strongly fractionated among meteoritic materials and it is well established that the most primitive C-rich meteorites also tend to have high N abundances (Kerridge, 1985). Nitrogen-bearing compounds are also a significant component of the carbonaceous material (CHON particles) sampled during the comet Halley encounter (e.g., Fomenkova et al., 1994). Large ^{15}N enrichments have been observed in whole rock samples, acid insoluble organic matter, solvent extractable organic compounds, and presolar grains (Messenger and Walker, 1997, and references therein). It has been suggested that the ^{15}N-rich material formed in the ISM and that the bulk of the acid insoluble carbonaceous matter in primitive chondrites was presolar in origin (Alexander et al., 1998). Previous studies have also implicated the carbonaceous material in IDPs as a likely host for the N (Stadermann et al., 1989; Aléon et al., 2003), and polycyclic aromatic hydrocarbons in particular (Clemett et al., 1993). Although -CN is commonly detected in spectra from the ISM and comets (e.g., Irvine et al., 1996) the EELS and FTIR data for the IDPs rule out a major C≡N component in these particles.

The IR and X-ray spectroscopic analyses of the D-poor yet ^{15}N-rich IDP (L2005*A3) implicate the remaining aromatic material in the particle as the host for the anomaly. Compared to related fragments from the same cluster, the aliphatic C-H stretches are extremely weak, while the XANES spectra are still dominated by C=C, most likely in ring structures. Additional support for this hypothesis comes from the observation of odd mass PAHs in other ^{15}N-rich IDPs that strongly suggests heteroatom functionality such as -NH_2 (Clemett et al., 1999).

The nature of the ^{15}N-rich host phase places strong constraints on the process that gave rise to its isotopic composition. It is likely that the high ^{15}N/^{14}N ratios are either a signature of stellar nucleosynthesis or extreme chemical mass fractionation. In the former case, the carrier would likely be a refractory mineral, such as the SiC or Si_3N_4 stardust found in meteorites (Anders and Zinner, 1993; Zinner 1998). However, as discussed above, there is no evidence for (>5 nm) crystalline phases in the N-bearing carbonaceous material in the N-rich IDPs (L2005*A3 and L2011R11). The N appears to be bound in a carbonaceous phase that, in principle, could have a stellar origin. However, any nucleosynthetic process resulting in elevated ^{15}N/^{14}N ratios would generally yield far greater C isotopic anomalies which have not been observed to date in IDPs (Messenger and Walker, 1997). Alternatively, the ^{15}N enrichment may have resulted from mass fractionation during chemical reactions at extremely low temperatures (chemical fractionation), which is known to be responsible for the high D/H ratios observed among many IDPs and primitive meteorites (McKeegan et al., 1985). In this case, the ^{15}N-rich phase ought to be bound in a chemical species or polymer, as is the case for the D-rich carrier. The present evidence favors chemical fractionation as the process which led to the high ^{15}N/^{14}N ratio in these IDPs. Owing to the small relative difference in the masses of ^{14}N and ^{15}N, the size of the N anomaly likely requires a formation temperature of <~30 K (Geiss and Bochsler, 1982). The conditions necessary to support chemical reactions at such low temperatures may only occur in cold molecular clouds (Geiss and Reeves, 1981). It is also interesting to note that UV photolysis of PAHs in NH_3-bearing ices results in the addition of N to the edges of the PAH molecules probably in the form of amine sidegroups (Sandford et al., 2001; Bernstein et al., 2002). Ion-molecule reactions in cold clouds are predicted to enrich NH_3 in ^{15}N (Terzieva and Herbst, 2000), and this mechanism provides a pathway for ^{15}N enrichment in the IDP aromatic hydrocarbons.

In several of the IDPs studied here, the D^- and ^{15}N-rich carbonaceous material serves as a matrix binding the other components of the IDP together (Fig. 11). It is tempting to conclude that the materials encased within presolar organic compounds are themselves presolar in origin. However, strong variations in the H and N isotopic compositions of IDPs suggest that this material has experienced variable degrees of processing. Furthermore, it is unclear at what stage these ma-

terials were brought together. The simplest case is represented by the rare, extremely anomalous D hotspots whose D/H ratios reach values of molecules in cold molecular clouds. It is possible that all of the materials observed within such hotspots are presolar in origin. In the one D hotspot successfully sliced and examined by TEM so far, only GEMS and carbonaceous material were observed. These grains may have served a role in the origin of the carbonaceous matter, either as sites for heterogeneous gas:solid reactions (Duley et al., 1989) or as substrates for the condensation of ices subsequently altered by radiation processes (Jenniskens et al., 1993; Bernstein et al., 1995). This hypothesis can now be tested through isotopic measurements of the grains embedded within D hotspots with the recently introduced NanoSIMS ion microprobe.

5. CONCLUSIONS

We studied a group of primitive anhydrous IDPs that exhibit a wide range of D/H ratios using combined ion microprobe, TEM, EELS, XANES and FTIR analyses and show that the D enrichments in IDPs are hosted by the abundant organic matter in these particles. Further constraints are provided by spectroscopic data showing that aliphatic hydrocarbons are a major host of the elevated D/H. The aliphatic hydrocarbons likely occur as branches or side bands on more complex macromolecular material. Based upon FTIR measurements, anhydrous IDPs typically have a higher ratio of aliphatic:aromatic functionality compared to primitive carbonaceous chondrite meteorites like Semarkona and Murchison.

Several of the IDPs in this study are enriched in N by a factor of ~3 over solar abundances and also show elevated $^{15}N/^{14}N$ ratios. The ^{15}N host is associated with the organic matter in these particles. Spectroscopic evidence indicates that the ^{15}N carrier is in the form of amine functionality attached to hydrocarbons, most likely aromatics. However, the high D/H and elevated ^{15}N reside in materials with different thermal stabilities, with the ^{15}N host being more refractory than the D-rich hydrocarbons.

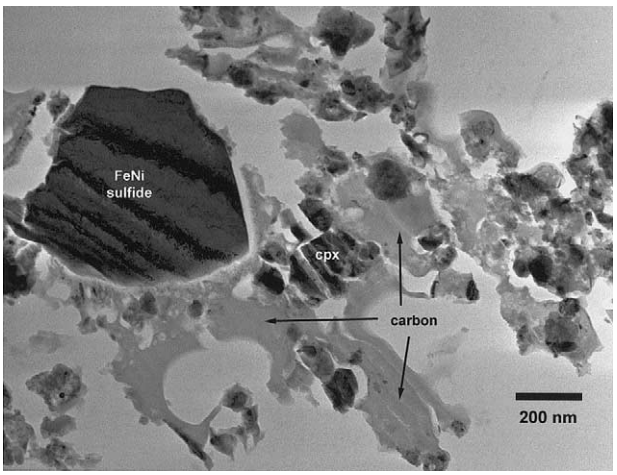

Fig. 11. A brightfield transmission electron image of the typical petrography in a thin section of L2011R11. The dark grains include both silicates and sulfides, while the abundant carbonaceous matrix material is indicated by arrows.

Table 2. Bulk elemental compositions of L2011R11, L2005*A3, L2008G12, L2008H9, and L2005#4 as determined by SEM-EDX techniques (see Thomas et al. 1993, for details of the analytical procedures, an example of the typical relative errors involved in these analyses are given in parentheses).

Element	L2011R11	L2005*A3	L2008G12	L2008H9	L2005#4
C	9.0 (1.0)	6.0	44.0	16.0	5.0
O	33.0 (1.0)	37.5	34.1	26.4	33.6
Na	1.6 (0.2)	4.0	0.6	0.9	7.5
Mg	9.9 (0.5)	9.7	2.9	7.4	10.1
Al	1.2 (0.2)	0.1	0.3	0.5	1.0
Si	15.2 (0.5)	12.9	11.2	17.4	12.8
P	0.6 (0.3)	0.3	0.9	0.3	0.4
S	8.0 (0.3)	7.5	1.0	8.8	4.7
Ca	0.9 (0.2)	0.8	0.1	0.8	0.6
Cr	0.2 (0.1)	0.1	n.d.	0.3	0.1
Mn	0.2 (0.1)	0.1	n.d.	0.3	0.1
Fe	19.2 (1.3)	19.9	5.0	19.0	20.6
Ni	1.0 (0.2)	0.9	0.3	2.1	0.9

Concentrations in atom %.

The D-rich aliphatic materials are volatilized or altered during atmospheric entry heating. The wide variation in D/H reflects incomplete mixing of presolar and solar system materials in the anhydrous IDP parent bodies (comets), or the partial loss of a volatile, very D-rich phase during atmospheric entry heating, or most likely, a combination of the two. Fig. 11. Table 2.

Acknowledgments—This work was supported in part by NASA RTOP 344-31-40-07 (LPK) and a NASA Cosmochemistry Program Grant NAG5-4843 (GJF). Portions of this research were carried out at the National Synchrotron Light Source, which is supported by the US Department of Energy, Division of Materials Sciences and Division of Chemical Sciences, under Contract No. DE-AC02-98CH10886. We thank K. Thomas-Keprta for the SEM-EDX bulk compositional analyses of some of the IDPs discussed in this manuscript. We thank Scott Sandford, Larry Nittler and Jerome Aléon for thoughtful and constructive reviews of the manuscript.

Associate editor: R. Wieler

REFERENCES

Aléon J., Engrand C., Robert F., and Chaussidon M. (2001) Clues to the origin of interplanetary dust particles from the isotopic study of their hydrogen-bearing phases. *Geochim. Cosmochim. Acta* **65,** 4399–4412.

Aléon J., Robert F., Chaussidon M., and Marty B. (2003) Nitrogen isotopic composition of macromolecular organic matter in interplanetary dust particles. *Geochim. Cosmochim. Acta* **67,** 3773–3787.

Alexander C. M. O., Russell S. S., Arden J. W., Ash R. D., Grady M. M., and Pillinger C. T. (1998) The origin of chondritic insoluble organic matter: A carbon and nitrogen isotope study. *Meteorit. Planet. Sci.* **33,** 603–622.

Allamandola L. J., Sandford S. A., and Tielens A. G. G. M. (1992) Infrared spectroscopy of dense clouds in the C-H stretch region: Methanol and diamonds. *Ap. J.* **399,** 134–146.

Anders E. and Grevesse N. (1989) Abundances of elements: Meteoritic and solar. *Geochim. Cosmochim. Acta* **53,** 197–214.

Anders E. and Zinner E. K. (1993) Interstellar grains in primitive meteorites: Diamond, silicon carbide, and graphite. *Meteoritics* **28,** 490–514.

Arpigny C., Jehin E., Manfroid J., Hutsemékers D., Schulz R., Stüwe J. A., Zucconi J.-M., and Ilyn I. (2003) Anomalous nitrogen isotope ratio in comets. *Science* **301,** 1522–1524.

Berger S. D., Bruley J., Brown L. M., and McKenzie D. R. (1989) Applications of the near-edge and low-loss fine structure in the analysis of diamond. *Ultramicroscopy* **28,** 43–46.

Bernstein M. P., Sandford S. A., Allamandola L. J., Chang S., and Scharberg M. A. (1995) Organic compounds produced by photolysis of realistic interstellar and cometary ice analogs containing methanol. *Ap. J.* **454,** 327–344.

Bernstein M. P., Sandford S. A., Allamandola L. J., Gillette J. S., Clemett S. J., and Zare R. N. (1999) UV irradiation of polycyclic aromatic hydrocarbons in ices: Production of alcohols, quinines, and ethers. *Science* **283,** 1135–1138.

Bernstein M. P., Elsilia J. E., Dworkin J. P., Sandford S. A., Allamandola L. J., and Zare R. N. (2002) Side group addition to the polycyclic aromatic hydrocarbon coronene by ultraviolet photolysis in cosmic ice analogs. *Ap. J.* **576,** 1115–1120.

Bradley J. P. (1994) Chemically anomalous, preaccretionally irradiated grains in interplanetary dust from comets. *Science* **265,** 925–929.

Bradley J. P. and Brownlee D. E. (1992) An interplanetary dust particle linked directly to type CM meteorites and an asteroidal origin. *Science* **251,** 549–552.

Bradley J. P., Brownlee D. E., and Veblen D. R. (1983) Pyroxene whiskers and platelets in interplanetary dust—Evidence of vapour phase growth. *Nature* **301,** 473–477.

Bradley J. P., Sandford S. A., and Walker R. M. (1988) Interplanetary dust particles. In *Meteorites and the Early Solar System* (eds. J. F. Kerridge and M. S. Matthews), pp. 861–898. University of Arizona Press, Tucson.

Bradley J. P., Keller L. P., Thomas K. L., and Brownlee D. E. (1993) Carbon analyses of IDPs sectioned in sulfur and supported on beryllium films. *Lunar Planet. Sci.* **24,** 173–174 [abstract].

Bradley J. P., Keller L. P., Snow T., Flynn G. J., Gezo J., Brownlee D. E., Hanner M. S., and Bowie J. (1999) An infrared 8-12 μm spectral match between GEMS and interstellar amorphous silicates. *Science* **285,** 1716–1718.

Brownlee D. E., Joswiak D. J., Schlutter D. J., Pepin R. O., Bradley J. P., and Love S. G. (1995) Identification of individual cometary IDPs by thermally stepped He release [abstract]. *Lunar Planet. Sci.* **26,** 183–184.

Charnley S. B. and Rodgers S. D. (2002) The end of interstellar chemistry as the origin of nitrogen in comets and meteorites. *Ap. J.* **569,** L133–L137.

Chiar J. E., Tielens A. G. G. M., Whittet D. C. B., Schutte W. A., Boogert A. C. A., Lutz D., van Dishoeck E. F., and Bernstein M. P. (2000) The composition and distribution of dust along the line of sight toward the Galactic center. *Ap. J.* **537,** 749–762.

Clemett S. J., Maechling C. R., Zare R. N., Swan P. D., and Walker R. M. (1993) Identification of complex aromatic molecules in individual interplanetary dust particles. *Science* **262,** 721–725.

Clemett S. J., Messenger S., Keller L. P., Zare R. N. (1999) Are aromatic hydrocarbons the carriers for D/H and 15N/14N isotope anomalies [abstract]. *Lunar Planet. Sci*. **30,** #1783 (CD-ROM).

Cody G., Alexander C. M. O., and Tera F. (2002) Solid-state (1H and 13C) nuclear magnetic resonance spectroscopy on insoluble organic residue in the Murchison meteorite: A self-consistent quantitative analysis. *Geochim. Cosmochim. Acta* **66,** 1851–1865.

Duley W. W., Jones A. P., and Williams D. A. (1989) Hydrogenated amorphous carbon-coated silicate particles as a source of interstellar extinction. *Mon. Not. R. Astron. Soc.* **236,** 709–725.

Ehrenfreund P., Robert F., D'Hendecourt L., and Behar F. (1991) Comparison of interstellar and meteoritic organic matter at 3.4 microns. *Astron. Astrophys.* **252,** 712–717.

Feser M., Wirick S., Flynn G. J., and Keller L. P. (2003) Combined carbon, nitrogen and oxygen XANES spectroscopy on hydrated and anhydrous interplanetary dust particles [abstract]. *Lunar Planet Sci*. **34,** #1875 (CD-ROM).

Flynn G. J., Sutton S. R., Bajt S., Klock W., Thomas K. L., and Keller L. P. (1993) The volatile content of anhydrous interplanetary dust [abstract] . *Meteoritics* **28,** 349–350.

Flynn G. J., Keller L. P., Jacobsen C., Wirick S., and Miller M. A. (1999) Organic carbon from interplanetary dust [abstract]. *Geophys. Res. Abstr*. **1 (*3*),** 751.

Flynn G. J., Keller L. P., Jacobsen C., and Wirick S. (2003) The origin of organic matter in the solar system: Evidence from the interplanetary dust particles. *Geochim. Cosmochim. Acta* **67,** 4791–4806.

Fomenkova M. N., Chang S., and Mukhin L. M. (1994) Carbonaceous components in the comet Halley dust. *Geochim. Cosmochim. Acta* **58,** 4503–4512.

Franke R., Bender S., and Hormes J. (1995) N K-shell absorption spectra of ionic and molecular crystals. *Phys. B* **208,** 293–294.

Fraundorf P., Lyons T., and Schubert P. (1982) The survival of solar flare tracks in interplanetary dust silicates on deceleration in the Earth's atmosphere. *J. Geophys. Res.* **87,** A409–A412.

Geiss J. and Reeves H. (1981) Deuterium in the Solar System. *Astron. Astrophys.* **93,** 189–199.

Geiss J. and Bochsler P. (1982) Nitrogen isotopes in the Solar System. *Geochim. Cosmochim. Acta* **46,** 529–548.

Irvine W. M., Bockelee-Morvan D., Lis D. C., Matthews H. E., Biver N., Crovisier J., Davies J. K., Dent W. R. F., Gautier D., Godfrey P. D., Keene J., Lovell A. J., Owen T. C., Phillips T. G., Rauer H., Schloerb F. P., Senay M., and Young K. (1996) Spectroscopic evidence for interstellar ices in comet Hyakutake. *Nature* **383,** 418–420.

Jenniskens P., Baratta G. A., Kouchi A., de Groot M. S., Greenberg J. M., and Strazzulla G. (1993) Carbon dust formation on interstellar grains. *Astron. Astrophys.* **273,** 583–600.

Keller L. P. (1998) A transmission electron microscope study of iron-nickel carbides in the matrix of the Semarkona unequilibrated ordinary chondrite. *Meteorit. Planet. Sci.* **33,** 913–919.

Keller L. P, and Flynn G. J. (2003) Far-IR spectroscopy of interplanetary dust, circumstellar silicate analogs and aerogel: A prelude to stardust samples [abstract]. *Lunar Planet. Sci*. **34,** #1903 (CD-ROM).

Keller L. P., Thomas K. L., and McKay D. S. (1992) An interplanetary dust particle with links to CI chondrites. *Geochim. Cosmochim. Acta* **56,** 1409–1412.

Keller L. P., Thomas K. L., Bradley J. P., and McKay D. S. (1995) Nitrogen in interplanetary dust particles [abstract]. *Meteoritics* **30,** 526.

Keller L. P., Thomas K. L., and McKay D. S. (1996) Carbon petrography and the chemical state of carbon and nitrogen in IDPs [abstract]. *Lunar Planet. Sci.* **27,** 659–660.

Keller L. P., Messenger S., Miller M., and Thomas K. L. (1997) Nitrogen speciation in a ^{15}N-enriched interplanetary dust particle [abstract]. *Lunar Planet. Sci*. **28,** #1811.

Keller L. P., Messenger S., and Bradley J. P. (2000) Analysis of a deuterium-rich interplanetary dust particle (IDP) and implications for presolar material in IDPs. *J. Geophys. Res. Space Phys.* **105,** 10397–10402.

Keller L. P., Hony S., Bradley J. P., Bouwman J., Molster F. J., Waters L. B. F. M., Brownlee D. E., Flynn G. J., Henning T., and Mutschke H. (2002) Identification of iron sulphide grains in protoplanetary disks. *Nature* **417,** 148–150.

Kerridge J. F. (1985) Carbon, hydrogen and nitrogen in carbonaceous chondrites: Abundances and isotopic compositions in bulk samples. *Geochim. Cosmochim. Acta* **49,** 1707–1714.

McKeegan K. D., Walker R. M., and Zinner E. (1985) Ion microprobe isotopic measurements of individual interplanetary dust particles. *Geochim. Cosmochim. Acta* **49,** 1971–1987.

Mennella V., Brucato J. R., Colangeli L., and Palumbo P. (2002) C-H bond formation in carbon grains by exposure to atomic oxygen: the evolution of the carrier of the interstellar 3.4 micron band. *Ap. J.* **569,** 531–540.

Messenger S. (1997) *Combined Molecular and Isotopic Analysis of Circumstellar and Interplanetary Dust*. Ph.D. dissertation, Washington University, St. Louis.

Messenger S. (2000) Identification of molecular cloud material in interplanetary dust particles. *Nature* **404,** 968–971.

Messenger S. and Walker R. M. (1997) Evidence for molecular cloud material in meteorites and interplanetary dust. *AIP Conf. Proc.* **402,** 545–564.

Messenger S., Keller L. P., Walker R. M., and Thomas K. L. (1996) Nitrogen petrography in two 15N-rich IDPs [abstract]. *Meteorit. Planet. Sci.* **31,** 88.

Messenger S., Stadermann F. J., Floss C., Nittler L. R., and Mukhopadhyay S. (2003a) Isotopic signatures of presolar materials in interplanetary dust. *Space Sci. Rev.* **95,** 1–10.

Messenger S., Keller L. P., Stadermann F. J., Walker R. M., and Zinner E. (2003b) Samples of stars beyond the Solar System: Silicate grains in interplanetary dust. *Science* **300,** 105–108.

Millar T. J., Bennett A., and Herbst E. (1989) Deuterium fractionation in dense interstellar clouds. *Ap. J.* **340,** 906–920.

Nittler L. R. (1996) *Quantitative Isotopic Ratio Imaging and Its Application to Studies of Preserved Stardust in Meteorites*. Ph.D. dissertation, Washington University, St. Louis.

Pendleton Y. J., Sandford S. A., Allamandola L. J., Tielens A G. G. M., and Sellgren K. (1995) Near infrared absorption spectroscopy of interstellar hydrocarbon grains. *Ap. J.* **437,** 683–696.

Pendleton Y. J. and Allamandola L. J. (2002) The organic refractory material in the diffuse interstellar medium: Mid-infrared spectroscopic constraints. *Astrophys. J. Suppl. Ser.* **138,** 75–98.

Rietmeijer F. J. M. (1992) Interplanetary dust particle L2005T12 directly linked to type CM chondrite petrogenesis. *Lunar Planet. Sci. Conf.* **23,** 1153–1154 [abstract].

Robert F. and Epstein S. (1982) The concentration and isotopic composition of hydrogen, carbon and nitrogen in carbonaceous meteorites. *Geochim. Cosmochim. Acta* **46,** 81–95.

Sandford S. A., Allamandola L. J., Tielens A. G. G. M., Sellgren K., Tapia M., and Pendelton Y. (1991) The interstellar C-H stretching band near 3.4 microns: Constraints on the composition or organic material in the diffuse interstellar medium. *Ap. J.* **371,** 607–620.

Sandford S. A., Bernstein M. P., Allamandola L. J., Gillette J. S., and Zare R. N. (2000) Deuterium enrichment of polycyclic aromatic hydrocarbons by photochemically induced exchange with deuterium-rich cosmic ices. *Ap. J.* **538,** 691–697.

Sandford S. A., Bernstein M. P., and Dworkin J. P. (2001) Assessment of the interstellar processes leading to deuterium enrichment in meteoritic organics. *Meteorit. Planet. Sci.* **36,** 1117–1133.

Shenoy S. S., Whittet D. C. B., Chiar J. E., Adamson A. J., Roberge W. G., and Hassel G. E. (2003) A test case for the organic refractory model of interstellar dust. *Ap. J.* **591,** 962–967.

Stadermann F. J., Walker R. M., and Zinner E. K. (1989) Ion microprobe measurements of nitrogen and carbon variations in individual IDPs. *Meteoritics* **24,** 327–328.

Stadermann F. J., Walker R. M., Zinner E. (1999) Sub-micron isotopic measurements with the Cameca NanoSIMS [abstract]. *Lunar Planet. Sci*. **30,** #1407 (CD-ROM).

Terzieva R. and Herbst E. (2000) The possibility of nitrogen isotopic fractionation in interstellar clouds. *Mon. Not. R. Astron. Soc.* **317,** 563–568.

Thomas K. L., Blanford G. E., Keller L. P., Klöck W., and McKay D. S. (1993) Carbon abundance and silicate mineralogy of anhydrous interplanetary dust particles. *Geochim. Cosmochim. Acta* **57,** 1551–1556.

Whittet D. C. B., Boogert A. C. A., Gerakines P. A., Schutte W., Tielens A. G. G. M., deGraauw T., Prusti T., van Dishoeck E. F., Wesselius P. R., and Wright C. M. (1997) Infrared spectroscopy of dust in the diffuse interstellar medium toward Cygnus OB2 No. 12. *Ap. J.* **490,** 729–740.

Zinner E. (1998) Stellar nucleosynthesis and the isotopic composition of presolar grains from primitive meteorites. *Annu. Rev. Earth Planet. Sci.* **26,** 147–188.